

ADC Characterization By Dynamic Integral Nonlinearity

Samer Medawar¹, Peter Händel^{1,2}, Niclas Björzell², Magnus Jansson¹

¹ *Signal Processing Lab, ACCESS Linnaeus Center, Royal Institute of Technology, SE-100 44 Stockholm, Sweden*

² *Department of Electronics, University of Gävle, SE-801 76 Gävle, Sweden*

Abstract- Wide band characterization of analog-digital converter integral nonlinearity (INL) based on parametric modeling and least-squares parameter fit is performed. In particular, the variations in the INL due to the frequency of the ADC stimuli are modeled. The INL is divided into two main entities describing the static and dynamic behavior of the ADC, respectively. The static component is modeled by a high code component (HCF) of piecewise linear segments centered around zero. A static low code (LCF) polynomial inherent to the INL data is added to the segments to complete the static part of the model. The INL dynamic part is modeled by an LCF polynomial. Method implementation is considered and is applied to 12-bit ADC data at 210 MSPS.

I. Introduction

An essential component of modern radio communication systems is the analog-digital converter (ADC). The ADC integral nonlinearity (INL) is a measure of how a practical ADC differs from a static ideal quantization staircase. Procedures how to measure INL are given in [1]. In this paper, dynamic characterization of INL is considered, where a parametric model is employed to represent the INL as a function of both ADC output code and test frequency.

Several models have been introduced in order to characterize the INL behavior [2–9]. Static high code frequency component (HCF) and low code frequency component (LCF) models were introduced in [2, 3]. The triangular wave stimuli was used to estimate the LCF in [4] and the HCF in [5], respectively. In [6], sine-waves were used to estimate both the LCF and HCF. In [9] the static LCF polynomial was identified when applying the method in [8] on measured ADC. The work [2–6] consider a static model for the INL. In this paper, we adopt the recent trend consisting of dividing the INL into the sum of a HCF and an LCF term, but also a dynamic model is considered as in [7–9].

In a first approximation, the INL is often regarded as a function of the output code only. Although, practical ADCs show a significant variation in the INL subject to a change in the test frequency. Thus, two dimensional, or dynamic models are required to fully describe the INL. In this paper, a model is developed, where the HCF component is represented by piecewise linear segments and the LCF component by a polynomial. The HCF describes the abrupt changes of the INL data that are related to the circuitry and design of the ADC. The LCF describes the smooth change with respect to the frequency. In [8], the segmented HCF was modeled by a first order polynomial. Here the linear segments are constrained to be centered around zero, in order to ensure a parsimonious model. Imposing these constraints, the number of HCF parameters are reduced by one half compared to the model employed in [8]. The polynomial representation is restricted to the LCF component. One merit of this new approach is the ability to identify a static polynomial in the LCF component. The LCF polynomials for different frequencies have similarities which are described by a static polynomial. This latter polynomial is added to the static HCF segments to represent the complete static attributes of the INL. A compact INL model data employing matrix notation is presented. A closed form solution is derived and endorsed by the implementation on simulated and measured ADC data.

This paper is organized as follows. We begin by explaining the INL model components in Section 2. The solution to the parametric estimation problem is presented in Section 3. The experimental set-up is outlined in Section 4. Implementation of the method on simulated and measured data is performed in Section 5. Section 6 concludes the paper.

II. INL Modeling

Finding a reliable method for characterizing the ADC is not a trivial task. In order to measure the INL, the plurality sine-wave test is used for its ease of implementation and reliability of results [1, §4.6]. The input signal spans the band

of interest, thus the sine-wave test stimuli generates an INL sequence for each test frequency. Basically, frequency stepping is done so a finite number of INL sequences is obtained. For INL-measurements test tone stimuli with frequency f_m Hz is used. The integer m represents the test frequency, so the test frequencies f_1, \dots, f_M are represented by $m = 1, \dots, M$.

Expressing the INL in terms of static HCF and dynamic LCF yields,

$$\text{INL}[m, k] = \text{HCF}[k] + \text{LCF}[m, k] \quad (1)$$

where k represents the digital output code of the ADC, m represents the test signal frequency f_m , $\text{HCF}[k]$ is the static high code frequency component and $\text{LCF}[m, k]$ the low code frequency component. The static term embedded in the LCF component is obtained by taking the mean of the polynomial data with respect to the frequency, that is

$$\text{SLCF}[k] \triangleq \frac{1}{M} \sum_{m=1}^M \text{LCF}[m, k] \quad (2)$$

By construction, the dynamic LCF polynomial is

$$\text{DLCF}[m, k] \triangleq \text{LCF}[m, k] - \text{SLCF}[k] \quad (3)$$

A full representation of the INL model is now given by

$$\text{INL}[m, k] = \underbrace{\text{HCF}[k] + \text{SLCF}[k]}_{\text{static part}} + \underbrace{\text{DLCF}[m, k]}_{\text{dynamic part}} \quad (4)$$

The INL representation in (1) is used for the derivation of the closed form solution to the parametric estimation problem.

The HCF components are related to the imperfections of the ADC quantizer for which the output is fairly independent of the frequencies within the bandwidth. The high code INL data $\text{HCF}[k]$ are modeled by piecewise linear segments centered around zero in order to deprive them of any polynomial attributes. So a specific code interval K_p is designed by:

$$\text{HCF}[k] \triangleq g[k, p] = \alpha[p] \left(k - \frac{k_{p-1} + k_p - 1}{2} \right) \quad (5)$$

where p refers to the ordered code interval

$$K_p : \{k | k_{p-1} \leq k < k_p\} \quad (6)$$

ranging from 1 to P . The output code has as a lower and upper end point, $k_0 = 1$ and $k_P = 2^N$, respectively. In the sequel N denotes the number of bits of the ADC. The set of regressor coefficients $\alpha[p]$ is gathered in a vector η of size P , that is

$$\eta = (\alpha[1], \dots, \alpha[P])^T \quad (7)$$

where T denotes transpose. Each component in η represents the slope of the zero centered segment. Note that, in [6] the notation $g[k, p]$ is introduced for the HCF-component. The dependency of $g[k, p]$ on both the output code k and segment p is convenient for the following discussion.

The LCF represents a smooth and continuous change of the INL data over the whole code range. The dynamic and static components constituting the LCF components are modeled by a polynomial of order L [3, 4, 6], that is

$$\text{LCF}[m, k] = h[k]^T \theta[m] \quad (8)$$

where $\theta[m]$ is a frequency dependent parameter vector

$$\theta[m] = (a_0[m], \dots, a_L[m])^T \quad (9)$$

and $h[k]$ is the regressor

$$h[k] = (1, k, \dots, k^L)^T \quad (10)$$

Let $y[m, k]$ denote the measured INL as function of code k and frequency f_m . Then, combining (5) and (8) one has

$$y[m, k] = g[k, p] + h[k]^T \theta[m] + e[m, k] \quad (11)$$

where $e[m, k]$ is introduced as a noise term that gather model imperfections, measurement noise, *et cetera* and is assumed to be a zero mean independent and identically distributed noise [8]. The model (11) describes how the measured INL $y[m, k]$ corresponding to test stimuli f_m and code k depends on the HCF $g[k, p]$ and LCF $h[k]^T \theta[m]$. Below, the problem of estimating the involved parameters (η in (7) and $\theta[m]$ in (9), for $m = 1, \dots, M$) is formulated and solved using matrix notation.

III. INL Parametric Estimation

Let m represent a test frequency f_m Hz for which the INL data is gathered in a vector \mathbf{y}_m , that is

$$\mathbf{y}_m = \begin{pmatrix} y[m, 1] \\ \vdots \\ y[m, 2^N - 1] \end{pmatrix} \quad (12)$$

Equation (11) can now be reformulated using matrix notation as

$$\mathbf{y}_m = \mathbf{g}\eta + \mathbf{h}\theta[m] + \mathbf{e}_m \quad (13)$$

where \mathbf{g} is a block diagonal matrix having the matrices \mathbf{g}_p on its diagonal, that is

$$\mathbf{g} = \text{blockdiag}(\mathbf{g}_1, \dots, \mathbf{g}_P) \quad (14)$$

The actual form of \mathbf{g}_p in (14) depends on the size and location of the segments (6). For $1 < p < P$ it holds that:

$$\mathbf{g}_p = \begin{pmatrix} -\frac{k_p - k_{p-1} - 1}{2} \\ \vdots \\ \frac{k_p - k_{p-1} - 1}{2} \end{pmatrix} \quad (15)$$

Segments $p = 1$ and $p = P$ have their first and end point at zero respectively. In order to model the LCF the Vandermonde matrix of dimensions $(2^N - 1) \times (L + 1)$ is introduced as

$$\mathbf{h} = \begin{pmatrix} 1^0 & 1^1 & \dots & 1^L \\ \vdots & \vdots & \ddots & \vdots \\ (2^N - 1)^0 & (2^N - 1)^1 & \dots & (2^N - 1)^L \end{pmatrix} \quad (16)$$

Using (16), the second term in (13) directly follows. Finally, \mathbf{e}_m in (13) is given by $\mathbf{e}_m = (e[m, 1], \dots, e[m, 2^N])^T$.

Since the input frequency is stepped in M steps over the whole bandwidth of interest, the multiple experiment data model yields

$$\begin{pmatrix} \mathbf{y}_1 \\ \vdots \\ \mathbf{y}_M \end{pmatrix} = \begin{pmatrix} \mathbf{g} & \mathbf{h} & & \\ & \vdots & \ddots & \\ & \mathbf{g} & & \mathbf{h} \end{pmatrix} \begin{pmatrix} \eta \\ \theta[1] \\ \vdots \\ \theta[M] \end{pmatrix} + \begin{pmatrix} \mathbf{e}_1 \\ \vdots \\ \mathbf{e}_M \end{pmatrix} \quad (17)$$

The INL data for each test frequency m is represented by a static piecewise linear segments component $\mathbf{g}\eta$ (same for all frequencies) and a polynomial $\mathbf{h}\theta[m]$.

By construction the HCF model has a piecewise linear behavior in consecutive segments. Thus a segmentation approach for the INL measurements $y[m, k]$ is needed. In this paper an adhoc method combined with manual intervention is employed. We foresee further work in this area in order to derive automatic segmentation procedures for INL characterization.

The solution to (17) can be derived by exploiting the inherent structure. Details can be found in [8]. The result reads

$$\hat{\eta} = \frac{1}{M} (\mathbf{g}^T \pi_{\perp} \mathbf{g})^{-1} \mathbf{g}^T \pi_{\perp} \sum_{m=1}^M \mathbf{y}_m = \mathbf{g}_{\pi_{\perp}}^{\dagger} \bar{\mathbf{y}} \quad (18)$$

where $\bar{\mathbf{y}}$ is the arithmetic average of the M data sets, that is

$$\bar{\mathbf{y}} = \frac{1}{M} \sum_{m=1}^M \mathbf{y}_m \quad (19)$$

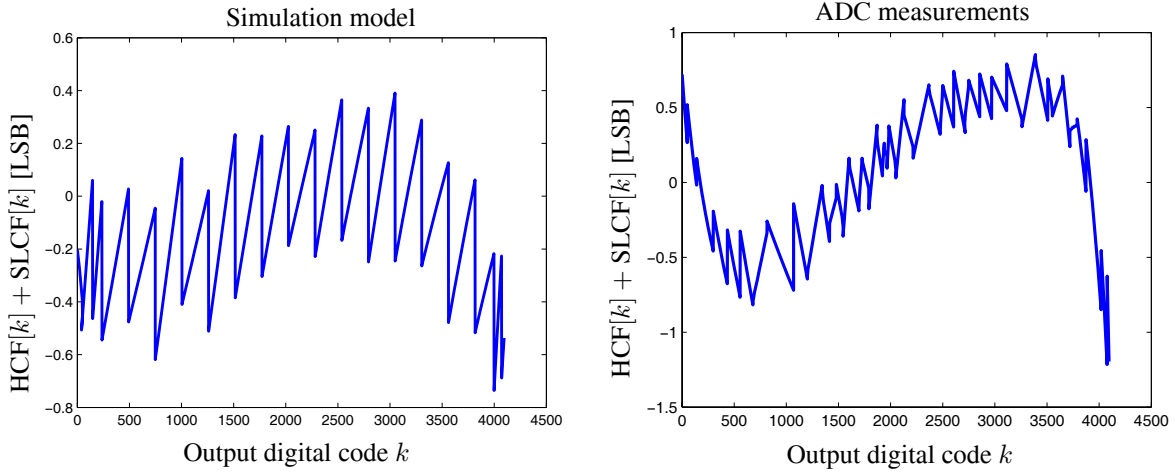
and $\pi_{\perp} = \mathbf{I} - \mathbf{h}(\mathbf{h}^T \mathbf{h})^{-1} \mathbf{h}^T$, with \mathbf{h} given in (16). Further, for each m ranging from 1 to M ,

$$\hat{\theta}[m] = (\mathbf{h}^T \mathbf{h})^{-1} \mathbf{h}^T (\mathbf{y}_m - \mathbf{g}\hat{\eta}) = \mathbf{h}_1^{\dagger} (\mathbf{y}_m - \mathbf{g}\hat{\eta}) \quad (20)$$

A brief summary of the problem statement and the method is presented in Table 1.

Table 1. INL characterization by vector notation

1)	Construct \mathbf{h} in (16)
2)	Determine the borders of the P HCF segments, and construct \mathbf{g} in (14) from the \mathbf{g}_p in (15)
3)	Collect the vector INL data $\mathbf{y}_1, \dots, \mathbf{y}_M$ corresponding to test frequencies f_1, \dots, f_M
4)	Calculate the HCF parameters $\hat{\eta}$ according to (18)-(19)
5)	For $m = 1$ to M : Calculate LCF parameters $\hat{\theta}[m]$ from (20)
6)	Calculate the the static LCF model in (2) as $\mathbf{g}\hat{\eta} + \mathbf{h}\bar{\theta}$ where $\bar{\theta}$ is the arithmetic average of $\hat{\theta}[m]s$
7)	For $m = 1$ to M : Calculate the dynamic LCF as $\mathbf{h}(\hat{\theta}[m] - \bar{\theta})$

**Fig. 1.** Static components of the ADC integral nonlinearity measured in LSBs as function of the output digital code k .

IV. Experimental Set-up

The ADC under test is a commercial 12-bit pipeline Analog Devices AD9430 intended for direct IF sampling that operates up to 210 MSPS conversion rate, having a measured spurious free dynamic range of -78.6 dB. The clock and input signals are generated by a high quality vector signal generator (VSG). Ultra low distortion and low noise IF amplifiers in combination with SAW filters and delay lines are used for signal conditioning in order to attenuate any potential spurious and harmonics generated by the VSG. The theoretical quantization noise for a 12 bit ADC is -74 dBFS (that is 74 dB lower than full scale), thus all the signals in use are verified (by the signal analyzer) to be at least -80 dBFS. The test frequencies spanned the range from 10 MHz to 90 MHz with a separation of 5 MHz making a total of 17 test signals. The power of each test signal is tuned to an approximate overload of 5 LSBs, which is the optimal input power to calculate the INL [10]. The measured data is saved and its INL is calculated by the method of sine fitting [1, §4.6]. Also, simulated AD9430 data is used. The simulation model is provided by the manufacturer (Analog Devices).

V. Results

The method outlined in Table 1 was applied on both simulated and measured data. As previously outlined, the static INL model is composed of two entities: HCF component (or segments) (5) and a static LCF polynomial denoted by $\text{SLCF}[k]$ according to (2). The complete static part of the data $\text{HCF}[k] + \text{SLCF}[k]$ is given in Figure 1 for the simulated and measured data, respectively.

We can note from Figure 1 that the static INL-model based on measured data is quite different from the one based on simulated data in the sense that the polynomial variation is more pronounced. The measured data required a polynomial of order $L = 7$ to achieve the model data fit while an order of $L = 3$ was enough for the data obtained

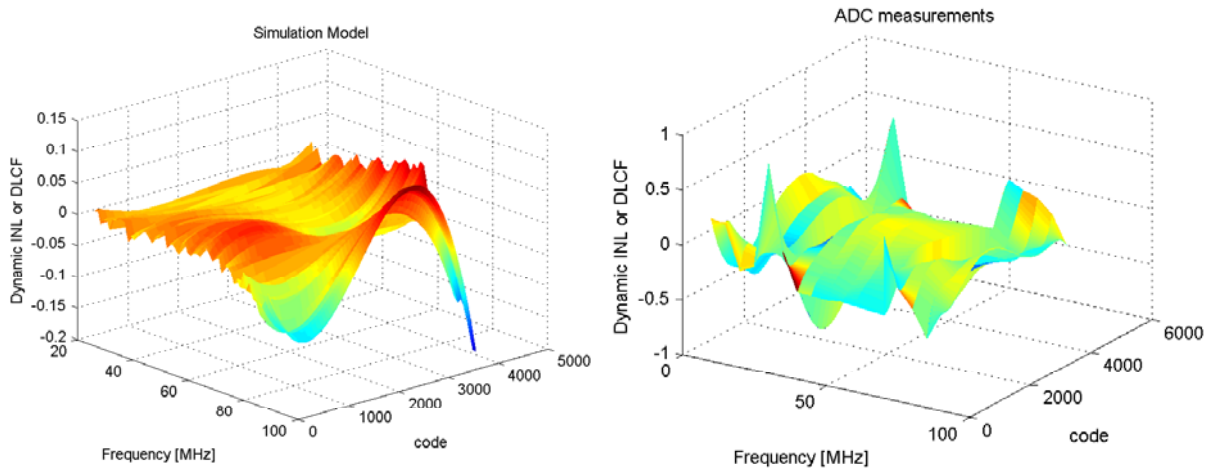


Fig. 2. Dynamic component of the LCF measured in LSBs as function of sine-wave test frequency f in MHz and output digital code k .

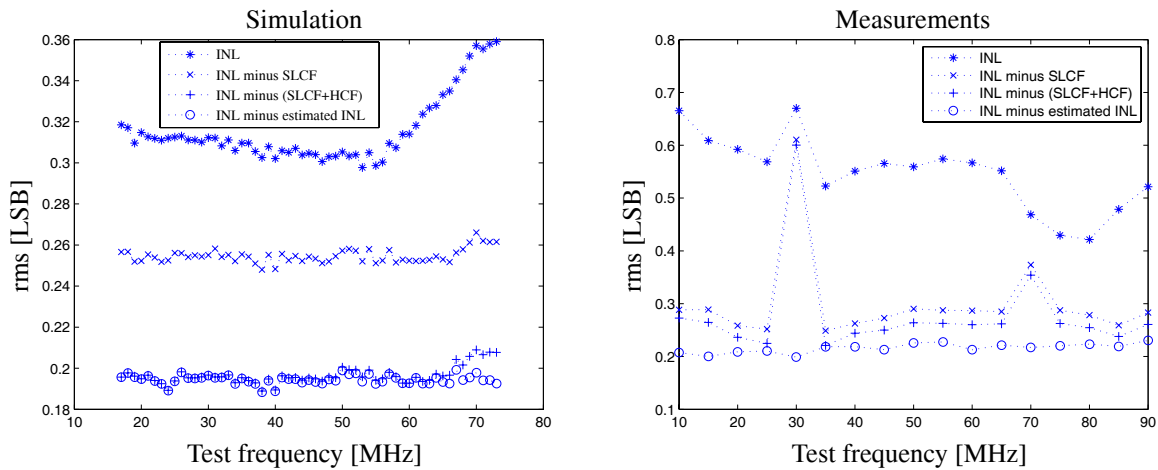


Fig. 3. rms of the INL data versus the rms error of the different estimated INL model components

from the simulation model. To comment more the data originating from the simulation model is more conform and structured than the measured one. The polynomial will tend to restrict the representation of the INL data structure (HCF plus LCF) in case its order is increased even more. In other words the segment structure will be included in the polynomial. These model orders are satisfactory at this stage, since they achieve a reasonable fit to the INL data.

The dynamic parts of the LCF components are plotted in Figure 2, using (3). The simulation model data tells that there exists some sensitivity to the frequency, while an ideal ADC should work indifferently regarding frequencies within the bandwidth. It is also obvious that the INL of the measured ADC data is more influenced by the frequency stimuli.

To study how the obtained models capture the INL-behavior the root-mean-square (rms) of the error $\mathbf{y}_m - \hat{\mathbf{y}}_m$ is studied in Figure 3. Here $\hat{\mathbf{y}}_m$ is the (vector) of model output when considering a static model based on the polynomial $\text{SLCF}[k]$ only, based on the static part $\text{SLCF}[k] + \text{HCF}[k]$, and the full model, respectively. The model error (in o) after subtracting the estimated INL model from the INL data is basically constant for all frequencies. Hence we have a fairly frequency independent rms-error, even if the rms of the INL data is relatively high at a certain test frequency.

Examining Figure 3 corresponding to simulated data, we can deduce that the static components ($\text{SLCF}[k]$ and $\text{HCF}[k]$) equally reduce the error since the (static) polynomial is of the same order in magnitude as the segments (Figure 1). The role of the dynamic component is not relevant until the higher test frequencies where the dynamic polynomial is more pronounced (see Figure 2). The same observation holds true for the measured data, the static components reduce the larger part of the error, but the proportions are not equal in this case. The $\text{SLCF}[k]$ has the most significant role in reducing the error since it is now larger in the magnitude than the segments (refer to Figure 1). A singularity is encountered at the 30 MHz measured data sequence, which could be due to a faulty measurement

or acquisition, or some spurious behavior that should be investigated more at this tone. The dynamic component contribution in reducing the error is small still, but it can be noticed over the whole test range due to the subsistence of relatively high dynamics (comparing to simulated data) for all the frequencies (see Figure 2).

VI. Conclusion

A dynamic modeling of ADC INL has been presented. The solution is derived using the least squares method. The static components is composed of HCF segments and an LCF polynomial, while the dynamic part is a low order polynomial. The static components showed to contain most of the INL information for the investigated ADC. The proposed INL model has a low complexity (typically some 50 parameters) and is suitable for post correction. The model captures a significant part of the INL, as illustrated in Figure 3.

VII. References

- [1] *IEEE Standard for Terminology and Test Methods for Analog-to-Digital Converters*, IEEE Standard 1241-2000.
- [2] L. Michaeli, P. Michalko and J. Saliga, "Identification of ADC error model by testing of the chosen code bins," *12:th IMEKO TC4 International Symposium*, September 25-27, 2002, Zagreb, Croatia.
- [3] L. Michaeli, P. Michalko, J. Saliga, "Unified ADC nonlinearity error model for SAR ADC," *Measurement*, Vol. 41, Issue 2, pp. 198-204, February 2008.
- [4] L. Michaeli, P. Michalko, and J. Saliga, "Identification of unified ADC error model by triangular testing signal," *10th Workshop on ADC modeling and testing*, Gdynia/Jurata, Poland, pp. 605-610, 2005.
- [5] A.C. Serra, M.F. da Silva, P.M. Ramos, R.C. Martins, L. Michaeli and J. Saliga, "Combined spectral and histogram analysis for fast ADC testing," *IEEE Transactions on Instrumentation and Measurement*, Vol. 54, No. 4, pp. 1617-1623, August 2005.
- [6] A. Cruz Serra, F. Alegria, L. Michaeli, P. Michalko, J. Saliga, "Fast ADC testing by repetitive histogram analysis," *IEEE Instrumentation and Measurement Technology Conference*, April 24-27, pp. 1633-1638, 2006.
- [7] N. Björzell and P. Händel, "Dynamic behavior models of analog to digital converters aimed for post-correction in wideband applications", *11th Workshop on ADC Modelling and Testing*, September 17-22, 2006, Rio de Janeiro, Brazil.
- [8] P. Händel, N. Björzell and M. Jansson, "Model based dynamic characterization of analog-digital-converters at radio frequency— Invited paper," *2007 International Conference on Signal Processing and its Applications*, 12-15 February 2007, Sharjah, UAE.
- [9] S. Medawar, N. Björzell, P. Händel and M. Jansson, "Dynamic characterization of analog-digital-converters nonlinearities," *Mosharaka International Conference on Wireless Communications and Mobile Computing*, Amman, Jordan 6-8 September 2007.
- [10] J. Blair, "Histogram measurement of ADC nonlinearities using sine waves," *IEEE Transactions on Instrumentation and Measurement*, vol. 43, no. 3, June 1994.
- [11] N. Björzell, O. Andersen, and P. Händel, "High dynamic test-bed for characterization of analogue-to-digital converters up to 500MSPS," *10th Workshop on ADC modeling and testing*, Gdynia, Poland, pp. 601-604, 2005.